J. exp. Biol. (1975), 62, 27–41
With 14 figures
Printed in Great Britain

APPLICABILITY OF HYDRODYNAMIC ANALYSES OF SPERMATOZOAN MOTION

By A. P. YUNDT, W. J. SHACK and T. J. LARDNER*
Massachusetts Institute of Technology

(*Received* 6 *May* 1974)

SUMMARY

This paper investigates the applicability of a simple hydrodynamics theory due to Gray & Hancock (1955), and extended by Brokaw (1970), to the analysis of the motions of sea urchin, rabbit, and bull spermatozoa. Experimental procedures for filming and analysing the swimming motions are presented. A detailed discussion of the agreement between the experimental and theoretical results is given, and the limitations of the theory in analysing the motion of mammalian spermatozoa are discussed.

INTRODUCTION

The quantitative analysis of the hydrodynamics of sperm motion began with the fundamental papers of Taylor (1951, 1952). However, Taylor's work was restricted to highly idealized forms of observed swimming motions. More realistic geometries were treated by Hancock (1953), but his method of analysis requires extensive numerical calculations and is unsuitable for direct application to experimentally observed motions. However the basic results of this analysis were subsequently used by Gray & Hancock (1955) to develop a simplified theory of flagellar swimming.

Brokaw (1970) recently has used the approach of Gray & Hancock to analyse arbitrary planar motions of a sperm tail. The bending moments in the sperm tail and the mechanical power dissipated by the swimming motion can be calculated using Brokaw's analysis in terms of the observed motion of the tail and a normal (C_N) and a tangential drag coefficient (C_T). It is possible to relate the form of these bending moments to the internal microstructure of the tail and to the energetics of motion; Brokaw (1972), for example, has presented a digital computer simulation of swimming sea urchin sperm based on such considerations (see also Blum & Lubliner, 1973). However, before we can have confidence in the physical parameters and accept the conclusions derived from such a simulation we must have confidence in the hydrodynamic analysis of Gray & Hancock from which bending moments are calculated.

This paper investigates the applicability of the theoretical hydrodynamic analysis to the quantitative description of the motion of both sea urchin and mammalian sperm. An investigation of this question was initiated by Brokaw (1970) in his analysis of the swimming motion of sea urchin (*Lytechinus pictus*) sperm. Although Brokaw

* Present address: Department of Theoretical and Applied Mechanics, University of Illinois, Urbana, Illinois.

analysed the motion of only two sea urchin sperm and discussed only the agreement between average propulsive velocities rather than a more detailed comparison, his results suggest '...that the hydrodynamic assumptions on which the computational methods are based are reasonably valid...A more thorough test of the hydrodynamic assumptions might be made by analysing a large number of photographs in a similar fashion.'

Brokaw compared average propulsive velocities to measure the agreement between the experiments and the theoretical analysis. For reasons to be discussed below, we have measured agreement by a comparison of the computed theoretical trajectory of the sperm with the experimentally observed trajectory.

The swimming motions of rabbit, bull, and sea urchin sperm were filmed following the procedures described in the next section. Tracings from these films were used to prepare input for the hydrodynamic analysis. In this paper we discuss the experimental results (for 250 msec elapsed time) for three sea urchin sperm (*Arbacia punctulata*), five rabbit sperm, and one bull sperm, and the comparison of these results with the hydrodynamic predictions. Our hydrodynamic formulation, with a number of modifications, follows that developed by Brokaw (1970).

A detailed discussion of the results for the sea urchin sperm is presented first. We found the 'noise' (i.e. random error) in our experimental data was sufficient to make meaningless any average speeds we computed directly from the raw data, so some data smoothing was necessary to obtain meaningful velocities. A detailed discussion of the numerical filtering techniques used is presented in Yundt (1974). We can conclude on the basis of agreement between the theoretical and experimental trajectories that Brokaw's analysis can provide good results for sea urchin spermatozoa.

We then present a discussion of rabbit and bull sperm for which the results for agreement between unsmoothed experimental and theoretical trajectories is not as good as for sea urchin spermatozoa. The smoothing techniques developed for the sea urchin sperm and the addition of head drag gave somewhat improved results. However, the agreement between these theoretical and experimental trajectories is still less satisfactory than for sea urchin spermatozoa although the basic trends indicated are correct.

This relatively poor agreement for mammalian sperm is discussed in terms of the limitations of the basic hydrodynamic assumptions of the simplified analysis. Our results suggest that the simple equilibrium analysis and experimental technique outlined here may be inadequate for the study of mammalian sperm. Further work is needed in the area of smoothing techniques for more meaningful analysis of experimental data. Further theoretical work is necessary on the various limitations of the simple hydrodynamic analysis, e.g. the effect of finite thickness of the tail, the effect of non-planar motion, end effects, and the interaction of swimming sperm either with each other or with nearby walls.

EXPERIMENTAL PROCEDURES

Several ripe male sea urchins (*Arbacia punctulata*) were obtained from the Marine Biological Laboratory of Woods Hole, Massachusetts, and kept cool and moist with sea water until needed for experiments. Sperm were obtained from a sea urchin by applying a one minute pulse of 12 volt r.m.s. alternating current across the genital

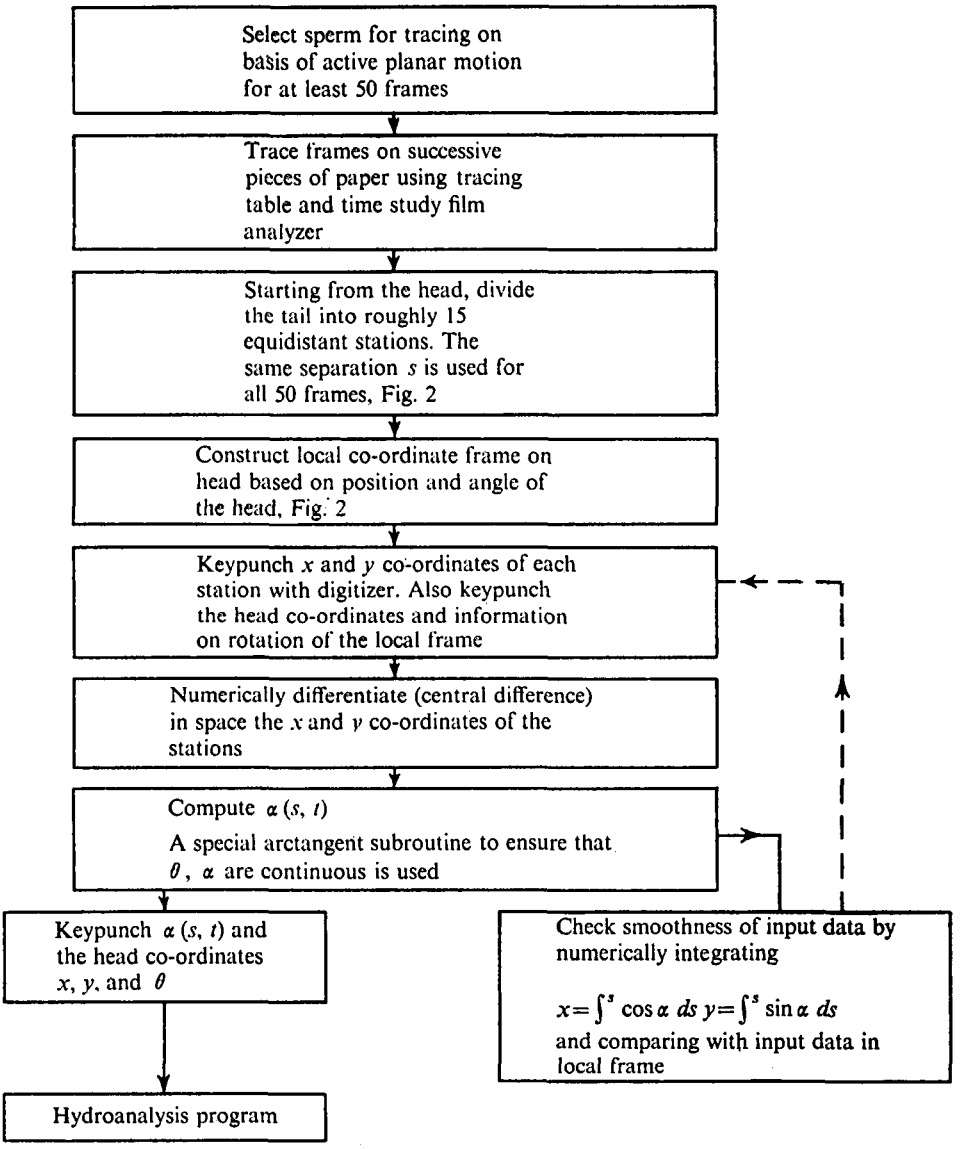

Fig. 1. Flow chart: Data handling prior to the hydrodynamic analysis program.

pores. The sea urchin was then placed, genital pores downward, on a beaker partially filled with sea water at room temperature into which the sea urchin discharged its semen. A drop of the resulting suspension was placed on a slide and covered. The sea urchin sperm were then filmed at 200 frames/sec on 16 mm Kodak 2498 film with a Locam camera (Redlake Labs, Santa Clara, California) through an American Optical microscope with a ×40 objective. A Zeiss 150 Watt xenon light source afforded enough illumination for high-speed film resolution, although a Zeiss heat filter was necessary to avoid heating the slide.

Mammalian sperm were studied with a different experimental procedure. The

reproductive tracts were dissected from New Zealand White rabbits killed by cervical dislocation. Frozen ejaculated bull sperm (Eastern Artificial Insemination Co-operative, Ithaca, N.Y.) were obtained extended in a routine mixture of 20% egg yolk, 7% glycerol, and a balance of 2·9% sodium citrate solution. Sperm from New Zealand White rabbits were also obtained by routine ejaculation of the bucks in an artificial vagina. The use of rabbit sperm from the epididymis rather than the ejaculate eliminated any influence by accessory gland fluids and afforded opportunity to study both mature and immature sperm.

The rabbit epididymis was dissected and minced in Hanks' Balanced salt solution (Microbiological Associates, Bethesda, Maryland). Portions of the head of the epididymis (containing immature sperm) or of the tail of the epididymis (containing mature sperm) were then minced in a few drops of Hanks' solution. Following additional dilutions with Hanks' solution, a drop of the mixture was placed on a slide and covered. Temperature during slide preparation was maintained at 37 °C with a slide warming tray. This entire slide preparation procedure takes less than 5 min.

The specimen was then filmed at 200 frames/sec with a Locam camera on either Kodak TriX reversal of Kodak 2498 film through a Zeiss microscope with a ×40 planachromat Nomarski objective. Again a Zeiss 150 W xenon light source was used for illumination, together with a Zeiss heat filter to avoid overheating the specimen. Temperature during microscopic examination was maintained at 37 °C with a Sage Air Curtain.

Preliminary data processing is summarized in Fig. 1. Complete movies were examined for individual sperm moving in planar fashion for a sequence of 50 frames (250 msec total elapsed time). A special tracing table was constructed to allow tracing these selected sequences on a fixed horizontal tablet. A time study projector permitted frame by frame tracing. The scale was determined by one frame of a film sequence of a Zeiss Objektmikrometer slide.

A local co-ordinate system was constructed for each frame traced to describe the position and orientation of the sperm tail. The origin of this local frame is the junction of the head and midpiece of the sperm, and the orientation is defined by an axis passing through the anterior tip of the head and the origin. This axis and its perpendicular form the local co-ordinate frame (see Fig. 2); by convention the positive x-axis points down the sperm tail and the positive y-axis is chosen so that the positive z-axis of a right-handed co-ordinate system comes 'out of the paper'. The origin is defined as station 1 and succeeding stations are evenly spaced along the tail separated by a constant distance Δs. Usually 10–15 stations proved adequate for numerical computation.

The co-ordinates of each station relative to a fixed co-ordinate frame denoted as X, Y were measured by a digitizer (Wayne-George T60 3610 X Y Co-ordicon) along with information about the origin and orientation of the local frame. A FORTRAN digital computer program was written which used the digitizer output to compute the tangent angles $\alpha(s, t)$ relative to the local frame at each station (i.e. for discrete values of s, the distance from the head measured along the sperm tail). This program also computed the head co-ordinates X, Y and θ, i.e. the position and orientation of the local frame in the global frame. These α angles and head co-ordinates formed the experimental input to the hydrodynamic analysis program.

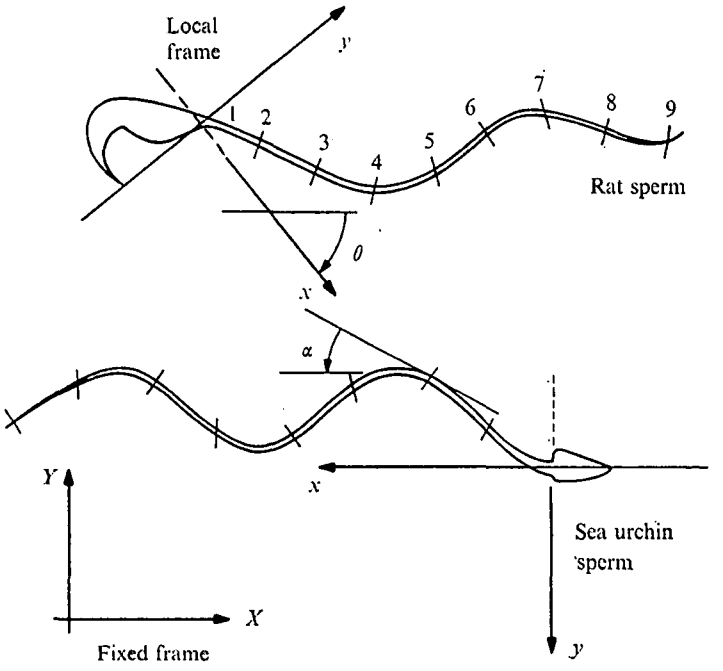

Fig. 2. Sample frame tracings showing local co-ordinates, stations and $\alpha(s,t)$.

ANALYSIS

Gray & Hancock (1955) and Brokaw (1970) have analysed the motion of planar swimming sperm and have obtained theoretical predictions for the propulsive velocity for a given motion of the sperm tail. In both these papers agreement between the theoretical analysis and experiment was measured by comparing the average theoretical and experimental propulsive velocities.

However, it is the trajectory of the sperm's motion which is directly measured experimentally, while the experimental propulsive velocity is computed by differentiation from these measurements.

Thus if $X(t)$ and $Y(t)$ are co-ordinates describing the motion of a point on the sperm head, the velocity components

$$V_X = \frac{dX}{dt}, \quad V_Y = \frac{dY}{dt}. \tag{1}$$

are obtained by calculating frame by frame differences in X and Y and dividing by the time increment between frames. This differentiation is difficult to do accurately since noise in the experimental trajectory measurements may give a spurious contribution to the experimental velocities.

If we denote the numerically computed velocities as V_{XN} and V_{YN} then

$$V_{XN} = V_X + \epsilon_X, \quad V_{YN} = V_Y + \epsilon_Y. \tag{2}$$

At any *instant* ϵ_X and ϵ_Y may be quite large due to the noise in the data, although their *average* values

$$\bar{\epsilon}_X = \frac{1}{T}\int_0^T \epsilon_X dt, \quad \bar{\epsilon}_Y = \frac{1}{T}\int_0^T \epsilon Y dt \tag{3}$$

may be quite small.

A straightforward computation of the instantaneous propulsive velocity V_N from equation (2) gives

$$\left.\begin{aligned} V_N &= \sqrt{(V_{XN}^2 + V_{YN}^2)} \\ &= \sqrt{[(V_X + \epsilon_X)^2 + (V_Y + \epsilon_Y)^2]} \end{aligned}\right\} \tag{4}$$

$$\simeq V[1 + (\epsilon_X V_X + \epsilon_Y V_Y)\ V^2 + (\epsilon_X^2 + \epsilon_Y^2)/2V^2], \tag{5}$$

where $V = \sqrt{(V_X^2 + V_Y^2)}$ is the true propulsive velocity and we have approximated the square root by the binomial theorem. Since the error in V_N depends on ϵ_X^2 and ϵ_Y^2, the random errors will no longer cancel in the averaging process. Different methods of computing the propulsive velocity and of filtering the data were examined, but no entirely satisfactory method was found: for details see Yundt (1974).

As will be discussed later, there is also a substantial component of noise in the experimental data describing the motion of the tail. Since the theoretical propulsive velocity is computed from this data, the theoretical propulsive velocity also has a spurious contribution from high frequency noise. If these spurious contributions to the average velocities are substantial, it may be misleading to compare them for agreement.

Instead of attempting to compute *instantaneous* frame by frame velocities, it is possible to compute average velocities over a number of frames. This greatly reduces the noise problem, but it seems inconsistent since the theoretical calculation is based on a frame by frame analysis of the tail motion. An instantaneous comparison of the trajectories was considered to be more satisfactory, since it could be done frame by frame but yet was much less sensitive to noise in the data.

An attempt was made to evaluate the contribution of noise to the experimental data by filming and analysing several dead sperm. The average velocity of these unmoving sperm was found to be on the order of 90 μm/sec when computed by using equation (4) directly. Since Brokaw (1965) gave the average velocity of a sea urchin sperm as being of the order of 150 μm/sec, the contributions from the noise to the average velocity is unacceptably large.

On the other hand, the computed theoretical trajectories of the dead sperm were contained in a 5 μm diameter circle. A motile sea urchin sperm might move as far as 40 μm in the same 250 msec period. Thus, the trajectory shows much less sensitivity to noise than does the average speed. If the high frequency noise contribution in experimental data taken from living sperm is similar to that found in dead sperm, agreement in trajectory may be more meaningful than agreement in average velocity.

A flow chart of the hydrodynamic analysis program is presented in Fig. 3. The basic formulation is due to Brokaw (1970). It is important to note that the program computes the trajectory when supplied with only the values of $\alpha(s, t)$ which describe the motion of the tail relative to the head, and the initial position of the sperm.

The swimming motions of the sea urchin spermatozoa chosen for analysis are illustrated by Figs. 4 and 5, which are composite tracings of every tenth frame (equivalent to a multiple exposure stroboscopic picture taken at 20 flashes/sec). These sperm are labelled sea urchin 1 (SU1), sea urchin 2 (SU2), and sea urchin 3 (SU3).

A typical plot for a sea urchin sperm showing $\alpha(s, t)$ versus time (frame number) at fixed x (station) is given in Fig. 6. The amplitude of $\alpha(s, t)$ versus time is typically increased at the end of the tail. Note the 'choppiness' indicative of noise in the data.

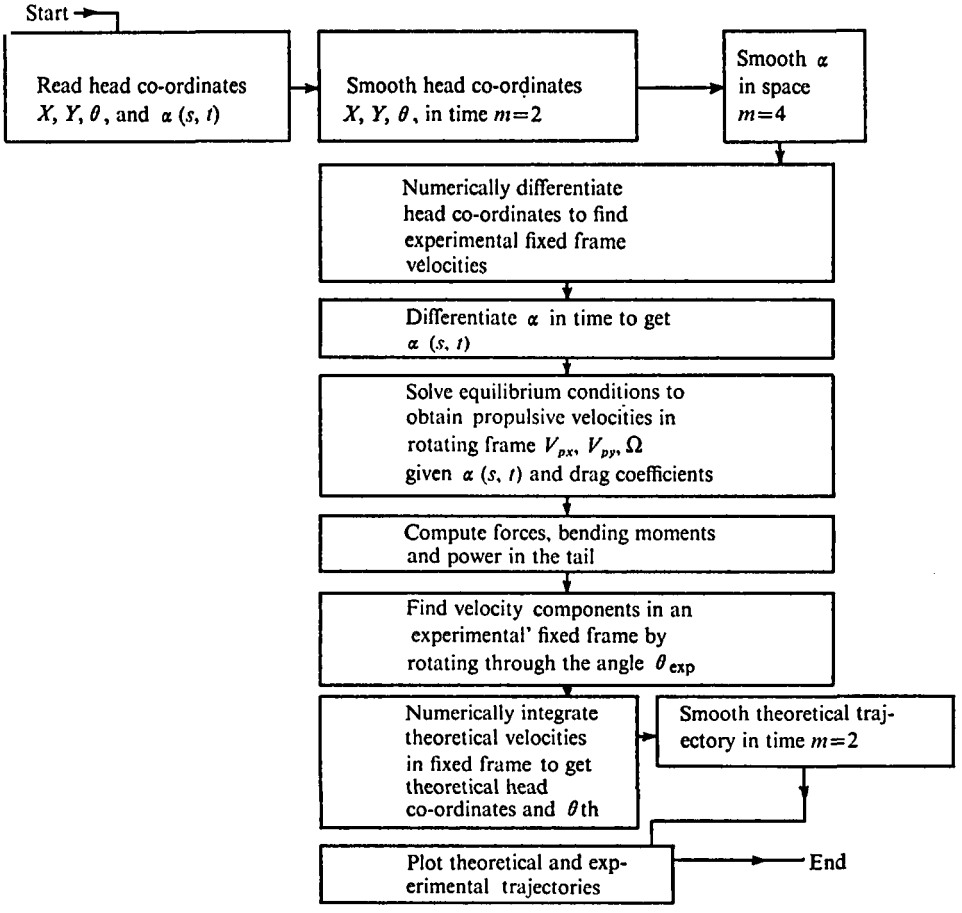

Fig. 3. Flow Chart: Hydrodynamic analysis.

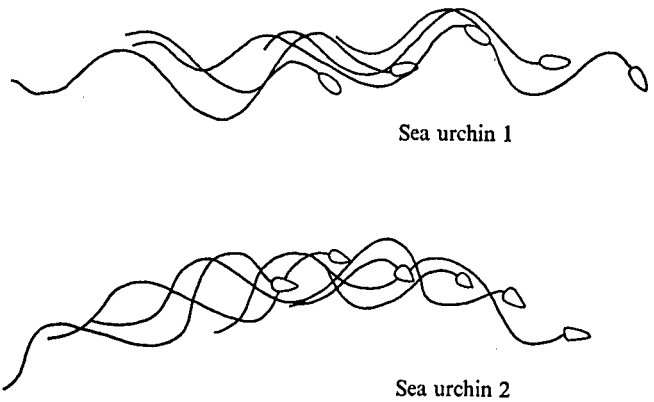

Fig. 4. Composite tracings of every tenth frame of sea urchin sperm 1 and 2.

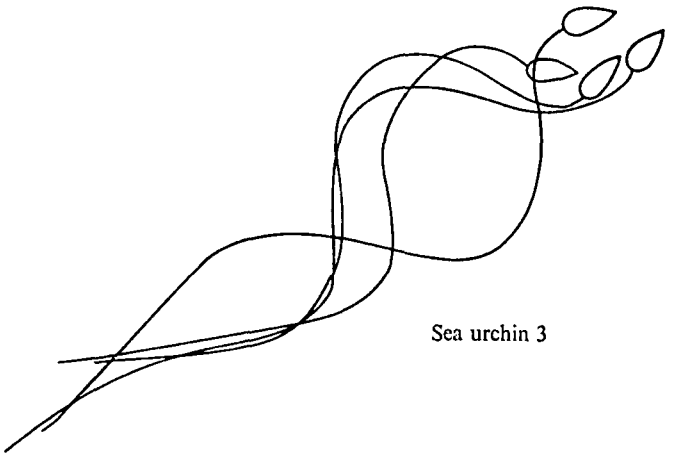

Fig. 5. Composite tracings of every tenth frame of sea urchin sperm 3.

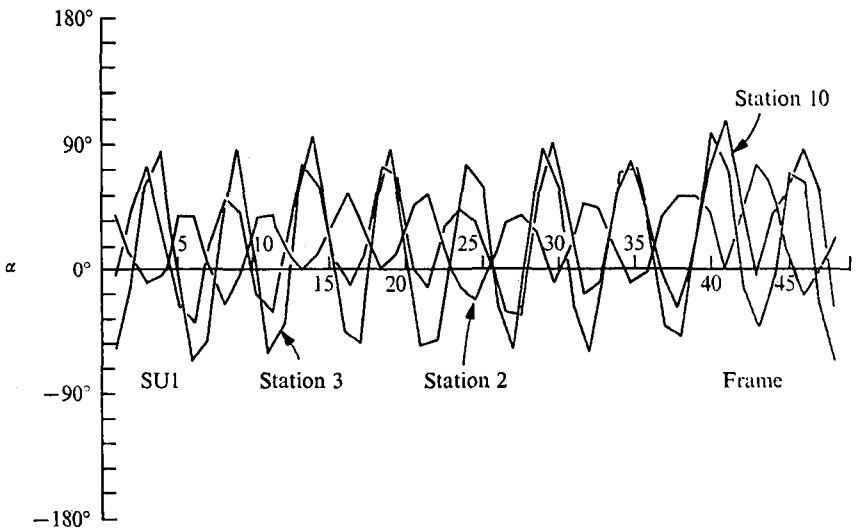

Fig. 6. $\alpha(s, t)$ versus time for sea urchin sperm 1.

A typical plot of $\alpha(s, t)$ versus s at a fixed time t is shown in Fig. 7. Note that $\alpha(s, t)$ is much smoother in space than in time.

The hydrodynamic analysis program solves the force and moment equilibrium equations for the propulsive velocity components V_{px} and V_{py} in the rotating local frame and for the rotational velocity Ω of the local frame fixed in the head (see Fig. 2 for description of local and fixed frames). These components may be transformed back into the fixed frame by using either a theoretically computed angle

$$\theta_{\text{th}}(t) = \theta_0 + \int_0 \Omega\, dt$$

or the experimentally measured angle θ_{exp}. If θ_{exp} rather than θ_{th} is used in the co-ordinate transform, errors in the theoretical trajectory may be attributed to errors in V_{px} and V_{py}, rather than to errors in some combination of V_{px}, V_{py}, and Ω. The

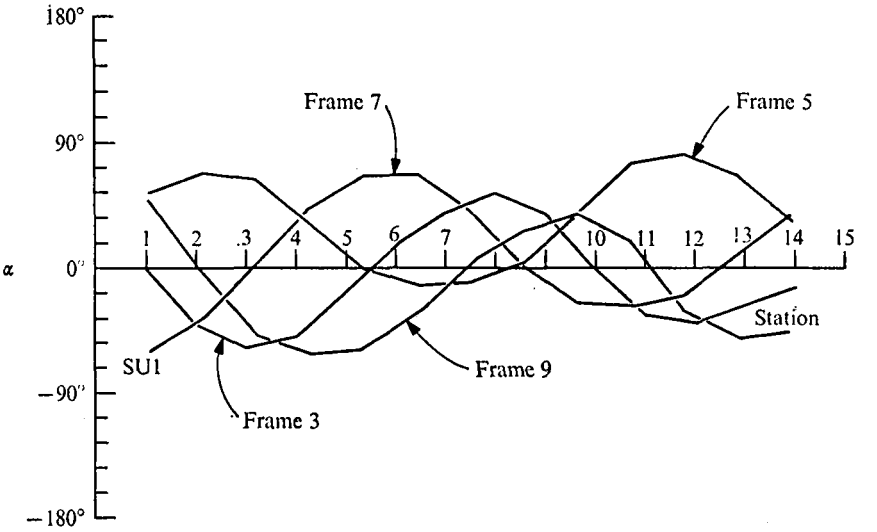

Fig. 7. $\alpha\,(s, t)$ versus station number for sea urchin sperm 1.

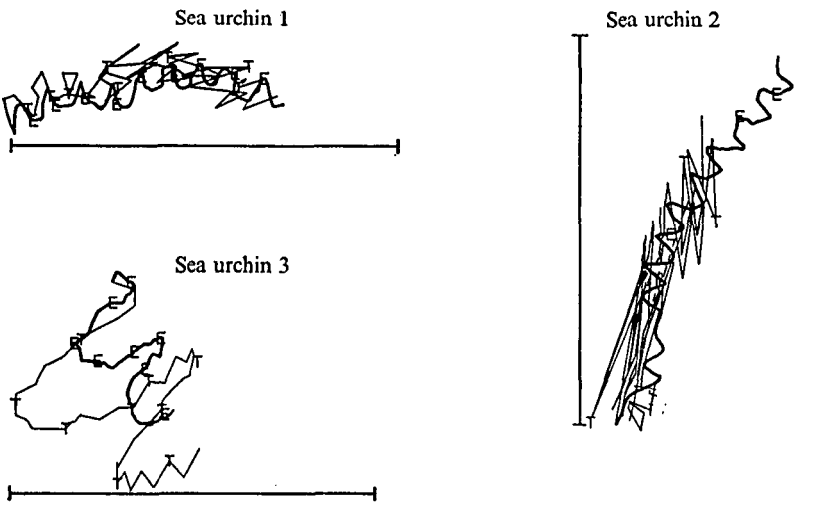

Fig. 8. Experimental and theoretical trajectories of sea urchin sperm 1, 2, and 3. Both trajectories are unsmoothed, $C_N/C_T = 2$, θ_{exp} used to compute theoretical trajectory. Bars are length of sperm tail (55 μm) to show relative amount of motion. Dark line is experimental trajectory.

differences in the trajectories computed by these two approaches are small. We have chosen to use θ_{exp} and examine the agreement between θ_{th} and θ_{exp} separately.

A comparison of the theoretically predicted and the experimentally observed trajectories of the sea urchin spermatozoa is given in Fig. 8. Fig. 9 compares θ_{th} and θ_{exp}.

The noise in the trajectories shown in Fig. 8 suggests a need for data smoothing. It is difficult to design a simple digital filter which eliminates the high frequency noise (somewhat arbitrarily defined as frequencies greater than 0·33 cycles/frame), while leaving unaltered the lower frequency signal components. Further work is needed,

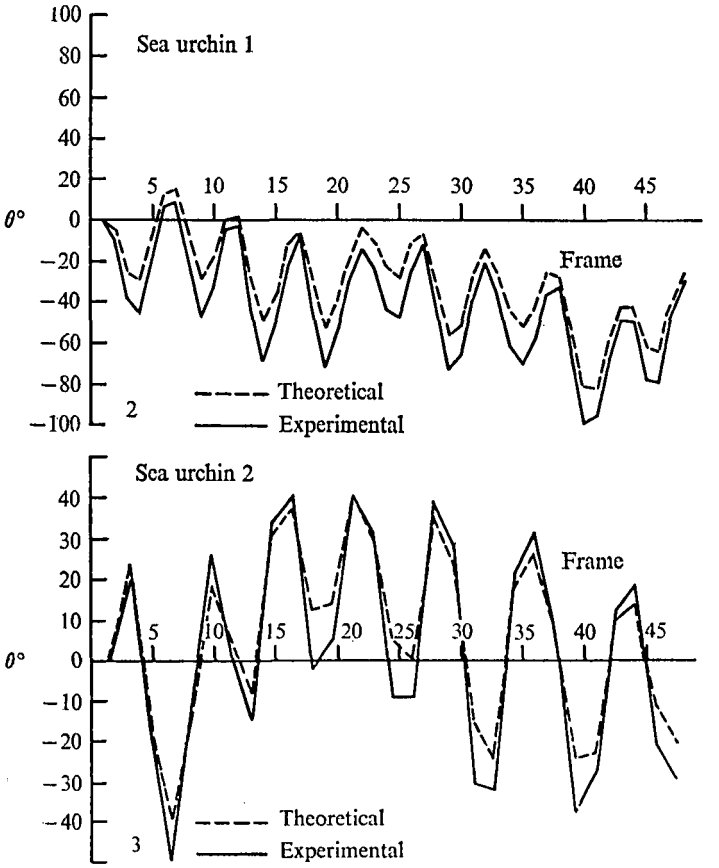

Fig. 9. Comparison of θ_{th} and θ_{exp} for sea urchin sperm.

perhaps using the inverse Fourier transform of a suitable modified spectrum, or a signal amplification stage in series with recursive low pass filtering.

The smoothing algorithm is a simple 'running mean', given by

$$x_n = \frac{x_{n-1} + mx_n + x_{n+1}}{m+2}, \tag{5}$$

where x_n is the nth smoothed value, x_{n-1}, x_n, and x_{n+1} are the $n-1$th, nth, and $n+1$th unsmoothed values, and m is an arbitrary coefficient. Filter coefficient $m = 4$ moderately smoothes higher frequencies only; smoothing with $m = 2$ eliminates/more high frequency noise but also attenuates the signal frequency band.

Further details on filters, smoothing techniques, and velocity definitions are given in Yundt (1974).

A standard smoothing procedure was developed in the computer program in which both the theoretical and experimental trajectories were smoothed through the use of equation (5). Fig. 10 shows the experimental and theoretical trajectories resulting from this standard smoothing technique.

The agreement for SU1 and SU2 is quite remarkable. Possible reasons for the poor agreement in the case of SU3 may be attributable to nonplanar motion and this will

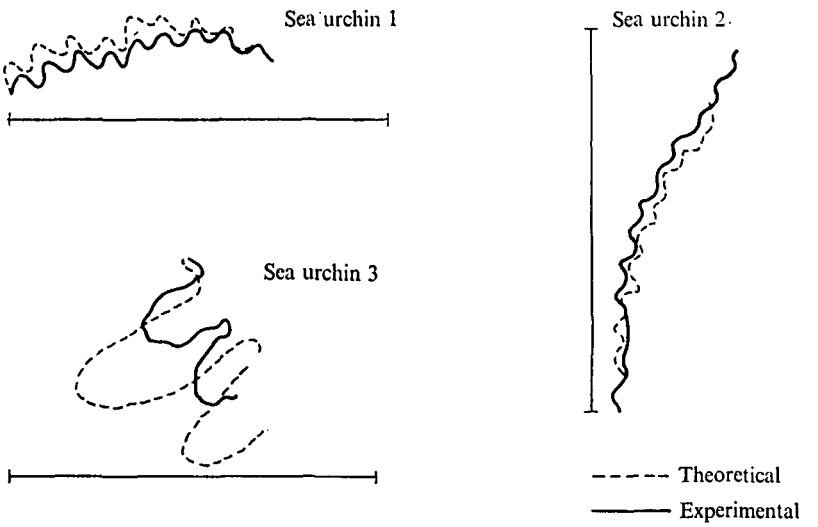

Fig. 10. Experimental and theoretical trajectories for sea urchin sperm. Bars represent the length of sea urchin sperm and dark line is the experimental trajectory.

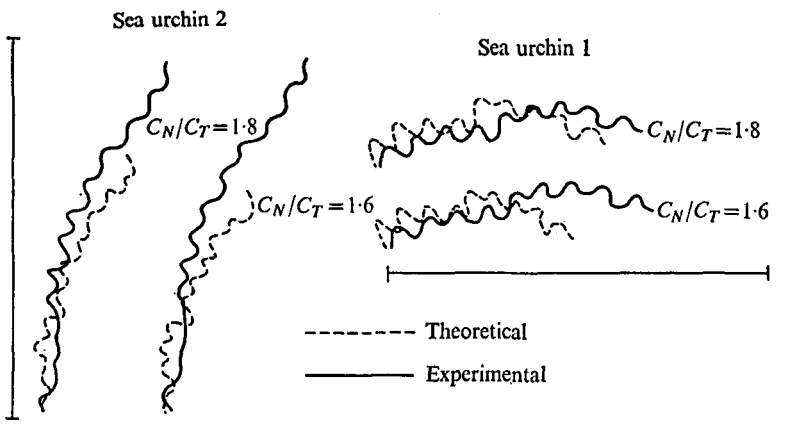

Fig. 11. Experimental and theoretical trajectories for sea urchin sperm 1 and 2 as the ratio C_N/C_T varies.

be discussed subsequently. We also note that SU3 has moved much less than SU1 and SU2 in the same time (see also Fig. 5).

After establishing a satisfactory data smoothing technique, we considered the choice of an appropriate value of the ratio C_N/C_T, ($C_N/C_T = 2$ for a vanishingly thin filament.) The data was smoothed using the standard smoothing technique and the program run with $C_N/C_T = 1{\cdot}8$ and $1{\cdot}6$. The resulting trajectories for SU1 and SU2 are shown in Fig. 11. Note the decrease in the total theoretical distance travelled when C_N/C_T decreases. This is not surprising since the proportion of drag in the direction of propulsion increases as C_N/C_T decreases.

Mammalian sperm may also be analysed using the techniques developed for sea urchin sperm. Mammalian sperm show a broader variety of motion than do sea urchin sperm, e.g. immature sperm (from the head of the epididymis) swim in a

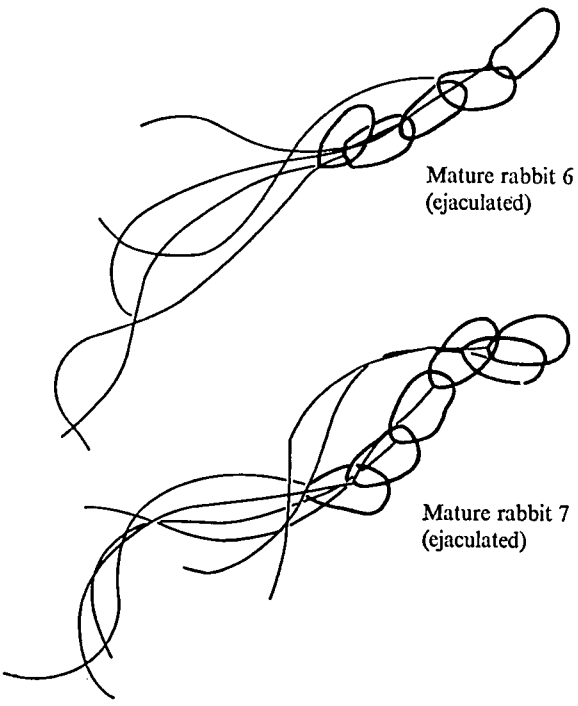

Fig. 12. Composite tracings of every tenth frame of mature rabbit sperm 6 and 7.

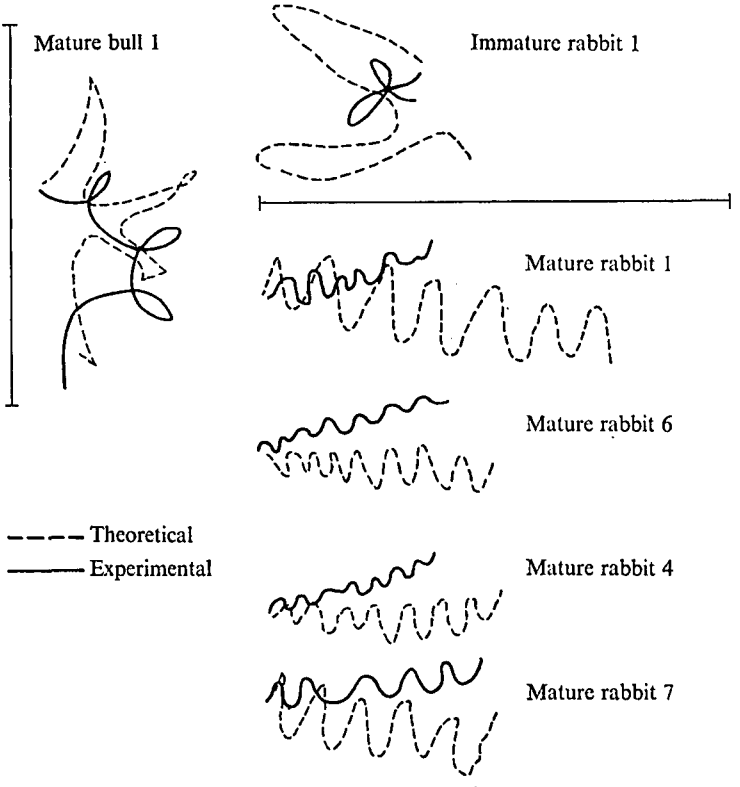

Fig. 13. Experimental and theoretical trajectories, $C_N/C_T = 2$ with no head drag. Bars represent length of sperm (Bull, 65 μm; Rabbit, 55 μm) and the dark line is the experimental trajectory.

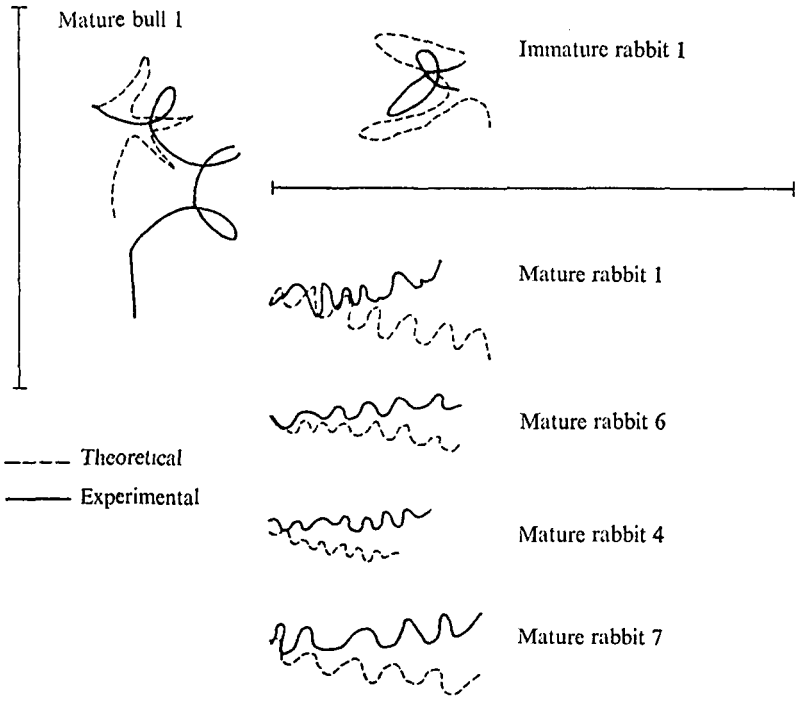

Fig. 14. Experimental and theoretical trajectories, $C_N/C_T = 2$ with head drag. Bars represent length of sperm (bull, 65 μm; rabbit, 55 μm) and the dark line is the experimental trajectory.

circular path while mature sperm (either from the ejaculate or from the tail of the epididymis) tend to swim in a roughly straight line (see Fray, Hoffer & Fawcett, 1972).

Experimental data taken from mammalian sperm also contain high frequency noise, so the standard smoothing technique discussed previously was used. Unfortunately, the theoretical trajectories did not agree as well with experiment for mammalian sperm as they did for sea urchin sperm.

We have analysed data from one ejaculated bull sperm, one immature rabbit sperm and four mature rabbit sperm. These sperm were labelled mature bull 1 (MBL1), immature rabbit 1 (IRB1), mature rabbit 1 (MRB1), mature rabbit 4 (MRB4), mature rabbit 6 (MRB6) and mature rabbit 7 (MRB7). Typical composite tracings of every tenth frame for two of these sperm are given in Fig. 12. Note the presence of much larger flagellar bends than in sea urchin sperm.

Plots of $\alpha(s, t)$ versus time for these sperm were obtained (Yundt, 1974); interpretation of these plots is the same as for sea urchin sperm: $\alpha(s, t)$ is relatively smooth in space but has a substantial component of high frequency noise in time.

The smoothed theoretical and experimental trajectories computed $C_N/C_T = 2{\cdot}0$ are shown in Fig. 13. Agreement is not as good as for sea urchin sperm. However, it is encouraging that the correct trends are present despite the irregular motion of the mammalian sperm.

When the drag of the head was taken into account, better agreement was obtained in many of the sperm as shown in Fig. 14. Head drag coefficients were estimated by

modelling the head as a flattened ellipsoid and using results presented by Happel & Brenner (1965); for details see Yundt (1974).

In our analysis of sea urchin sperm we were able to examine the effect of different values of the ratio C_N/C_T, and to select an optimal value. The agreement in analysis of mammalian sperm is not good enough to permit selection of optimal values of head drag coefficients of C_N/C_T from a similar examination of the effects of different values of head drag coefficients and C_N/C_T.

DISCUSSION

We have investigated the applicability of the simple equilibrium hydrodynamic analysis due to Gray & Hancock (1955) and extended by Brokaw (1970) to the motion of sea urchin, rabbit, and bull sperm. A comparison of experimentally measured and theoretically predicted motions was made to check the validity of the analysis. Experimental procedures for filming the swimming motions of sea urchin, rabbit, and bull sperm were developed. Film sequences of 50 frames (250 msec elapsed time) of the swimming motion of these sperm have been analysed.

Since our experimentally measured data contained a large proportion of noise, several dead sperm were filmed and analysed in order to measure the effects of noise on the analysis. From these studies we concluded that noise affected the velocity measurements much more than it did the trajectories. The large proportion of noise suggested that data smoothing was necessary to obtain meaningful results. A standard smoothing technique was developed which involved smoothing both experimental and theoretical trajectories in time and smoothing $\alpha(s, t)$ in space.

The results obtained for the sea urchin sperm indicated that at least in some cases theoretical and experimental agreement is sufficiently good to lend credence to the calculations of the bending moments within the flagella and of the power dissipated.

Data from mammalian sperm (rabbit and bull) processed with the standard smoothing technique did not show such satisfactory agreement. If the effects of head drag were added to the analysis, agreement was improved. Even though trajectory agreement was not as accurate as for sea urchin sperm, it was encouraging that the theoretical trajectories of mammalian sperm had the correct trends.

A possible explanation for the lack of good trajectory agreement in mammalian sperm is the inapplicability of the simple equilibrium analysis. This analysis assumes planar motion; however, it was noted during rabbit sperm tracing that portions of the tail would occasionally go out of focus, thus suggesting non-planar motion.

It is also possible that the hydrodynamic assumptions of the analysis are violated. The validity of the simple expression for viscous shear force in terms of the drag coefficients C_N and C_T depends on the 'thinness' of the tail. This thinness is measured in terms of the ratio d/L, where d is a characteristic diameter of the tail and L is a characteristic length of the tail. However, this ratio is of the order of $(10)^{-2}$ for sea urchin, bull and rabbit sperm, indicating equal validity of the hydrodynamic analysis to each sperm using this thinness criterion.

This indicates that probably the most important problem is the development of a satisfactory technique for the observation and measurement of non-planar motions. The hydrodynamic analysis appears to be satisfactory for the planar motion of sea urchin sperm. However, until the non-planar motions of mammalian sperm can be

analysed, it will be impossible to assess the hydrodynamic limitations of the simple equilibrium analysis for mammalian sperm. It is apparent from our results that a planar analysis based on these hydrodynamic principles is not satisfactory for mammalian sperm.

REFERENCES

BLUM, J. J. & LUBLINER, J. (1973). Biophysics of flagellar motility. *A. Rev. Biophys. Bioengng* **2**, 181–213.

BROKAW, C. J. (1965). Non-sinusoidal bending wave of sperms flagella. *J. exp. Biol.* **43**, 155–69.

BROKAW, C. J. (1970). Bending moments in free swimming flagella. *J. exp. Biol.* **55**, 289–304.

BROKAW, C. J. (1972). Computer simulation of flagellar movement 1. Demonstration of stable bend propagation and bend initiation by sliding filament model. *Biophys. J.* **12**, 564–86.

FRAY, C. S., HOFFER, A. & FAWCETT, D. (1972). A re-examination of motility patterns of rat spermatozoa. *Anat. Rec.* **173**, 301–8.

GRAY, J. & HANCOCK, G. J. (1955). The propulsion of sea urchin spermatozoa. *J. exp. Biol.* **32**, 802–14.

HANCOCK, G. J. (1953). The self-propulsion of microscopic organisms through liquids. *Proc. R. Soc. Lond.* A **217**, 96–121.

HAPPEL, J. & BRENNER, H. (1965). *Low Reynolds Number Hydrodynamics*, pp. 220–33. Englewood Cliffs, N.J.: Prentice Hall.

TAYLOR, G. I. (1951). Analysis of the swimming of microscopic organisms. *Proc. R. Soc. Lond.* A **209**, 447–61.

TAYLOR, G. I. (1952). The action of waving cylindrical tails in propelling microscopic organisms. *Proc. R. Soc. Lond.* A **211**, 224–39.

YUNDT, A. P. (1974). Applicability of simple equilibrium hydrodynamic analysis to the motion of sea urchin, rabbit, and bull sperm. Master of Science Thesis, Department of Mechanical Engineering, Massachusetts Institute of Technology, February 1974.